THE JOURNAL OF THE ACOUSTICAL SOCIETY OF KOREA VOL.23, NO.1E 2004. 3 pp. 3-9

Designing a Microphone Array for Acoustical Inverse Problems

Youngtea Kim*
Computational Science & Engineering Lab, Samsung Advanced Institute of Technology (SAIT)
(Received December 10 2003; accepted March 17 2004)

Abstract

An important inverse problem in the field of acoustics is that of reconstructing the strengths of a number of sources given a model of transmission paths from the sources to a number of sensors at which measurements are made. In dealing with this kind of the acoustical inverse problem, strengths of the discretised source distribution can be simply deduced from the measured pressure field data and the inversion of corresponding matrix of frequency response functions. However, deducing the solution of such problems is not straightforward due to the practical difficulty caused by their inherent ill-conditioned behaviour. Therefore, in order to overcome this difficulty associated with the ill-conditioning, the problem is replaced by a nearby well-conditioned problem whose solution approximates the required solution. In this paper a microphone array are identified for which the inverse problem is optimally conditioned, which can be robust to contaminating errors. This involves sampling both source and field in a manner which results in the discrete pressures and source strengths constituting a discrete Fourier transform pair.

Keywords: *Acoustical inverse problem, Condition number, Discrete Fourier transform*

I. Introduction

The principal purposes of source identification and quantification are to aid the selection of appropriate and cost-effective noise control, and to predict the noise in regions other than the measurement region. The application of source identification and, more generally, the reconstruction of acoustic source distributions from measurements at field points, has been a point of interest for many acousticians in recent years. Solution of the discrete inverse problem in acoustics can yield estimates of acoustic source strength from measurements of acoustic pressure in the radiated field. The basis of an approach to a typical inverse problem in acoustics is illustrated in Figure 1, which is a simple example of a free field radiation problem associated with a vibrating planar surface where no other sources or obstacles exist in the exterior region. The figure shows a diagrammatic representation of both the real source and measurement array, and the discretised model sources and modelled measurement array. Here, when it is assumed that the real source strength distribution is considered to consist of a finite number N of discrete elements (where, the source strengths comprise a complex vector $\mathbf{q}$), the modelled acoustic pressures $\mathbf{p}$ at the same number of discrete field points as model sources can be written in the discrete matrix form $\mathbf{p}=\mathbf{Gq}$, where the matrix $\mathbf{G}$ is assumed to be known from the model and represents the complex frequency response functions. The matrix $\mathbf{G}$ relates the complex vector of the model acoustic pressures $\mathbf{p}$ to the assumed complex vector of the discrete source distribution $\mathbf{q}$.

However, in practical applications contaminating errors of various kinds are inevitable. As illustrated in Figure 1,

Corresponding author: Youngtea kim (yt65.kim@samsung.com)
Computational Science & Engineering Lab, Samsung Advanced Institute of Technology (SAIT), Giheung-eup, Yongin-si, Gyeonggi-do, 449-712, Korea

these errors include noise due to measurement contamination of the complex acoustic pressure $\hat{\mathbf{p}}$ and errors involved in the model representation of the real source distribution. When assuming that the real source distribution produces acoustic pressures measured at a finite number N of receiver positions where the complex pressures detected comprise the elements of the vector $\hat{\mathbf{p}}$, the difference between the model pressures $\mathbf{p}$ and the measured pressures $\hat{\mathbf{p}}$ is expressed as the vector of complex errors. This is given by $\mathbf{e}=\hat{\mathbf{p}}-\mathbf{p}$. Therefore, the measured acoustic pressures $\hat{\mathbf{p}}$ at the discrete field points can be represented by

$$\hat{\mathbf{p}}=\mathbf{G}\mathbf{q}+\mathbf{e}. \tag{1}$$

Here, the estimate of the model source strength vector $\mathbf{q}$ is deduced by minimising the error criterion (which is also called the cost function). This is defined by $J=\|\mathbf{e}\|^2=\|\mathbf{G}\mathbf{q}-\hat{\mathbf{p}}\|^2$, where $\|\ \|$ denotes the 2-norm. Finally, the least squares estimate is given by[1, 2]

$$\mathbf{q}=\mathbf{G}^{+}\hat{\mathbf{p}}, \tag{2}$$

where the matrix $\mathbf{G}^{+}=[\mathbf{G}^{H}\mathbf{G}]^{-1}\mathbf{G}^{H}$ is the 'pseudo inverse' of the matrix $\mathbf{G}$, which reduces to $\mathbf{G}^{+}=\mathbf{G}^{-1}$ when the matrix $\mathbf{G}$ has a square dimension and is non-singular matrix (which is guaranteed if the matrix $\mathbf{G}$ is positive definite). The superscript H denotes Hermitian transpose.

For dealing with inverse problems of the type described here. it is very useful to introduce the SVD as the primary analytical tool. The usefulness of SVD stems from the fact that the complex matrix $\mathbf{G}$ (which, for this case, is assumed to be square but the more general case is discussed in references[1-2]) can be decomposed into the following product of the three matrices[3],

$$\mathbf{G}=\mathbf{U}\Sigma\mathbf{V}^{H}=\sum_{i=1}^{N}\mathbf{u}_i\sigma_i\mathbf{v}_i^{H}\ , \tag{3}$$

where the matrix $\mathbf{U}$ is a matrix of left singular vectors $\mathbf{u}_i$ of the matrix $\mathbf{G}$, and the matrix $\mathbf{V}$ is a matrix of right singular vectors $\mathbf{v}_i$ of the matrix $\mathbf{G}$. Both matrices $\mathbf{U}$ and $\mathbf{V}$ are unitary and have the properties $\mathbf{U}^{H}=\mathbf{U}^{-1}$ and $\mathbf{V}^{H}=\mathbf{V}^{-1}$. The $N\times N$ matrix Σ is simply diagonal; matrix whose diagonal elements σ_i comprise the singular values of the matrix $\mathbf{G}$ (i.e., $\sigma_1\geq\sigma_2\geq\cdots\cdots\geq\sigma_N\geq 0$). By substituting the transformed equation (3) provided by the SVD into equation (2), and by using the orthonormal properties of the unitary matrices $\mathbf{U}$ and $\mathbf{V}$, the least squares estimation of the acoustic source strength can be written as

$$\mathbf{q}=\mathbf{V}\Sigma^{+}\mathbf{U}^{H}\hat{\mathbf{p}}=\sum_{i=1}^{N}\frac{\mathbf{u}_i^{H}\hat{\mathbf{p}}}{\sigma_i}\mathbf{v}_i\ , \tag{4}$$

where the matrix Σ^{+} is the pseudo inverse of the matrix Σ and is given by $diag(1/\sigma_1,1/\sigma_2,\cdots\cdots,1/\sigma_N)$. As can be seen in equation (4), the very small singular values (compared to the largest singular value σ_1) of the matrix Σ to be inverted can produce large quantities of elements in the matrix Σ^{+}. This effect associated with the small singular values of the matrix $\mathbf{G}$ will introduce large errors into the solution deduced.

The most important attribute of the matrix $\mathbf{G}$ relating the behaviour of the small singular values is the *condition*

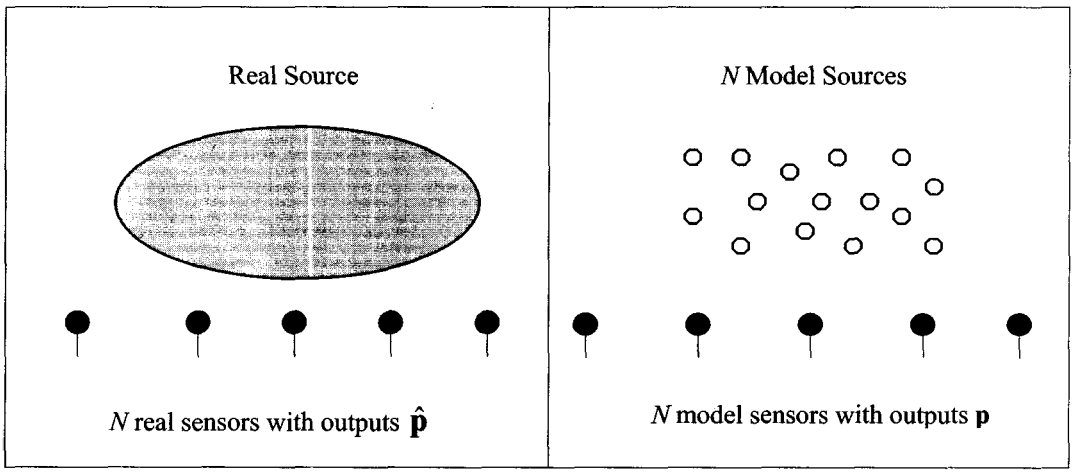

Figure 1. A schematic diagram for estimation of acoustic source distribution by the inverse technique based on the assumed source model.

number $\kappa(\mathbf{G})$ of the matrix. This is given by [3]

$$\kappa(\mathbf{G}) = \| \mathbf{G} \| \| \mathbf{G}^{-} \| . \tag{5}$$

This represents the ration between the largest and smallest nonzero singular values of the matrix **G**. The importance of the condition number $\kappa(\mathbf{G})$ results from the fact that it can be a measure of the sensitivity of the solution to errors in the matrix **G** itself or in the measured pressures $\hat{\mathbf{p}}$. For example, by using various properties of matrix norms, if the complex vector **p** changes to $\mathbf{p}+\delta\mathbf{p}$, the corresponding solution becomes $\mathbf{q}+\delta\mathbf{q}$ and then **G** $(\mathbf{q}+\delta\mathbf{q}) = \mathbf{p}+\delta\mathbf{p}$. The ratio of the norms of the relative changes can be shown to satisfy the inequality [3]

$$\frac{\|\delta\mathbf{q}\|}{\|\mathbf{q}\|} \le \kappa(\mathbf{G}) \frac{\|\delta\mathbf{p}\|}{\|\mathbf{p}\|} . \tag{6}$$

Here, small perturbations in the complex vector **p** and the matrix **G** to be inverted are amplified in the complex vector **q** by an amount directly proportional to the condition number $\kappa(\mathbf{G})$ of the matrix **G**. Thus, the matrix **G** is called ill- or well-conditioned according to $\kappa(\mathbf{G})$ being large or small. Hence when the matrix **G** has unit condition number in uncertain circumstances, the associated inverse problem is very easy to solve and the strengths of the elementary sources can be reliably estimated from the inversion of the Green function matrix **G**.

However, in practice if one wants to reconstruct precise and detailed source distribution by means of an approach based on the SVD considered in this paper, a real source needs to be discretised with a great number of modelled sources as many as possible and measurements have to be undertaken at least at the same number of sensors as modelled sources. In such cases, the acoustical inverse problem generally appear to be best conditioned when the number of sources and sensors are small[1, 2]. In other words, as the number of modelled sources and sensors increase, in general, the problem becomes very poorly conditioned and resulting in producing an inaccurate solution. In order to overcome the ill-condition, some numerical techniques are used[1-2]. However, the use of regularisation often suppresses the effect of small singular values in the frequency response function matrix to be inverted and these are in turn often associated with high spatial frequencies of the source distribution. Thus the numerical process produces a useful estimate of the acoustic source strength distribution but with a limited spatial resolution. Furthermore, unfortunately, the inter-source spacing of modelled sources for producing successful reconstruction is limited by the half-wavelength, even when prior knowledge of source distribution is revealed[2]. Therefore, it is the purpose of this paper to identify this particular condition in a simple 2D case and extend the result of this potentially useful observation to the 3D case.

II. The 2D Radiation Problem

Consider a typical radiation problem with a finite vibrating plate as shown in Figure 2. In such cases, it follows from the Rayleigh integral and the appropriate two-dimensional Green function that the far field acoustic pressure can be expressed as a spatial Fourier transform of the associated source distribution. This relationship is valid for kR ? 1 can be written as [4]]

$$p(\hat{k}) = G_c(kR) \int_{-\infty}^{\infty} u_z(x) e^{j\hat{k}x} dx , \tag{7}$$

where $G_c(kR) = \omega\rho_o e^{-jkR}/2\pi R$ (where the wavenumber $k = \omega / c_0$, where ω is the angular frequency and c_0 is the sound speed) and ρ_0 is the density. $u_z(x)$ is the velocity normal to the x-axis and the wavenumber variable $\hat{k} = k\sin\theta$. Equivalently, sensors at the radial distance R can be spaced at equal increments of $\hat{k} = k\sin\theta$ as depicted in Figure 3(a).

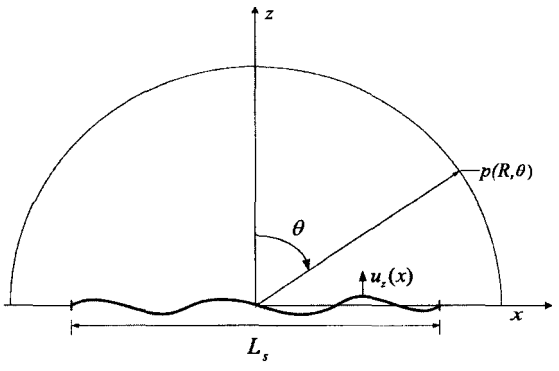

Figure 2. Continuous far field pressures on the hemi-cylinder with radius R.

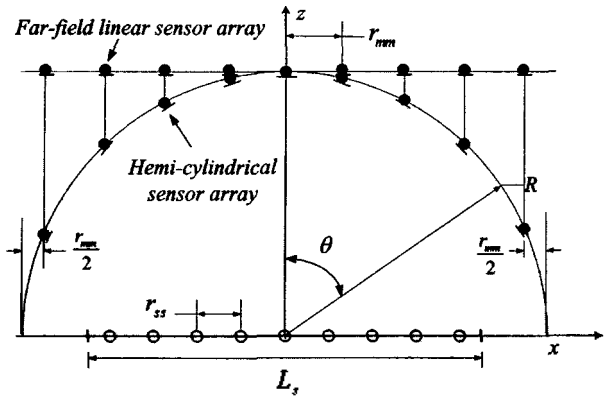

(a) The far-field linear sensor array with equal inter-sensor spacing r_{mm} for the hemi- cylindrical sensor array.

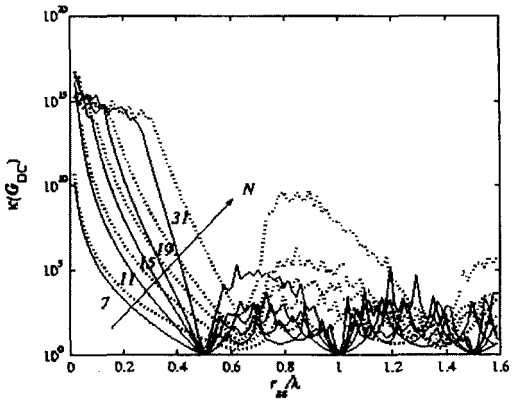

(b) Variation of the condition number for the hemi-cylindrical sensor array (solid line) and the far-field linear sensor array (dotted line) where, N denotes the number of model sources and sensors

Figure 3. The hemi-cylindrical sensor array and the far-field linear sensor array, when $R = 10^3 r_{ss}$.

In order to consider how the sensor array can be optimally spaced, one must firstly understand the relationship between the spatial Fourier transform of the far field data and the spatial Fourier transform of the source distribution. Similarly, by the analogous argument to that given for the sampling of time histories (see, for example, reference[5] for a full discussion), the discrete spatial Fourier transform of a source distribution of a finite length can be deduced. Now, as depicted in Figure 3 (a), assume that only N points have non-zero source strength in the interval $[-L_s/2,\ L_s/2]$ and these points are equally spaced with an increment of $r_{ss}(=L_s/N)$. The sampling points in $[-L_s/2,\ L_s/2]$ are defined as

$$x_n = -\left(\frac{L_s - r_{ss}}{2}\right) + nr_{ss}, \qquad n = 0,\ 1,\ \cdots\cdots,\ N-1 \tag{8}$$

In this case, the continuous variable $u_z(x)$ is replaced by the discrete variable $u_z(x_n)$, and then the discrete Fourier spectrum of the spatially sampled source strength distribution $u_z(x_n)$ can be expressed in the form

$$U_z(\hat{k}) = \frac{1}{\sqrt{N}} \sum_{n=0}^{N-1} u_z(x_n) e^{jkr_n}, \tag{9}$$

where $U_z(\hat{k})$ is a sequence of length N. Now note that the spatial frequency range of $\hat{k}$ between $-k$ and k can be split into N samples for evaluation of $U_z(\hat{k})$ at N specific values of spatial frequencies with an increment of $2\pi/Nr_{ss}$. This in turn implies that $2\pi/Nr_{ss} = 2k/N\,(=\Delta\hat{k})$ from which it follows that $r_{ss} = \lambda/2$ since $k = 2\pi/\lambda$. Therefore, the Fourier spectrum at each of $m(2\pi/Nr_{ss})$ values of the spatial frequency, where m is the index associated with each discrete spatial frequency chosen (which is defined as $m = 0,\ 1,\ \cdots\cdots,\ N-1$), can be written as

$$U_z(m\Delta\hat{k}) = \frac{1}{\sqrt{N}} \sum_{n=0}^{N-1} u_z(x_n) e^{j(2\pi nm/N)}. \tag{10}$$

Thus, using the discrete Fourier spectrum of the spatially sampled source distribution given by equation (10), the far field acoustic pressure in equation (7) can be written as

$$p(m\Delta\hat{k}) = G_c(kR) \sum_{n=0}^{N-1} \frac{1}{\sqrt{N}} u_z(x_n) e^{j(2\pi nm/N)}, \tag{11}$$

which demonstrates that they are a discrete Fourier transform pair[6]. Note that this is accomplished by sampling the far field pressure at M equal increments of $\sin\theta$. In matrix terms the above equation can be written $\mathbf{p} = G_c(kR)\mathbf{W}\mathbf{u}$, where

$$\mathbf{W} = \frac{1}{\sqrt{N}} w^{(r-1)(s-1)}, \quad r,s = 1,2,\cdots\cdots,N, \tag{12}$$

where $w = e^{j2\pi/N}$ and N denotes the number of discretised points. In equation (12), W is the Fourier matrix which has singular values that are all unity [3], and thus the condition number of the matrix W has a ratio of maximum to minimum singular value of unity.

Figure 3(b) shows that the conditioning of the matrix $\mathbf{G}_{DC}(=G_c(kR)\mathbf{W})$ for the hemi-cylindrical sensor array which has the discrete Fourier transform relationship with the spatially sampled source distribution as described in above, when the sensor array is placed in the far field (for example, when $r_{ms}=10^3 r_{ss}$). As illustrated in this figure, by the adoption of the far-field linear sensor array depicted in Figure 3(a) the conditioning of the matrix $\mathbf{G}_{DC}$ is worse in a wide region of r_{ss}/λ as the number of the assumed sources increases. The sensor array is located at the distance R from the sources with the same inter-sensor spacing r_{mm} as that of the hemi-cylindrical sensor array. However, the conditioning of the matrix $\mathbf{G}_{DC}$ for the hemi-cylindrical sensor array becomes optimal (i.e., has a condition number of unity) when $r_{ss}/\lambda=0.5$, irrespective of the number of sources and sensors assumed. In other words, the hemi-cylindrical sensor array will have the least sensitivity to contaminating errors when $r_{ss}/\lambda=0.5$, and the errors resulting from its inversion defined in equation (4) are therefore at a minimum. This may be the case in particular in uncertain circumstances which usually occur due to practical difficulties in obtaining prior knowledge of either noise contamination or the source distribution.

III. The 3D Radiation Problem

It has been noted in a previous section that, for a particular 2D acoustic radiation problem, the matrix of Green functions relating the sampled far field acoustic pressure to the strengths of a discrete array of elementary acoustic sources has unit condition number at a certain frequency. The associated inverse problem is thus very easy to solve at this frequency and the strengths of the elementary sources can be reliably estimated from the inversion of the Green function matrix. It is valuable to explore this relationship further and extend the result of this potentially useful observation to the 3D case.

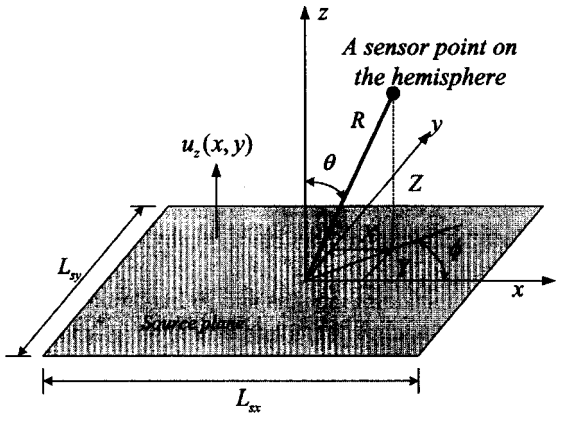

Figure 4. Sensor points on the hemisphere of radius R.

Consider a three-dimensional example with the set of planar sources. The three dimensional relationship between the spatial Fourier transform of the far field acoustic pressure on the hemisphere with radius R and the spatial Fourier transform of the associated planar source distribution is given by Rayleigh's first integral formula,

$$p(k_x,k_y)=G_s(kR)\int_{-\infty}^{\infty}\int_{-\infty}^{\infty}u_z(x,y)\,e^{j(k_x x+k_y y)}dxdy, \tag{13}$$

where $G_s(kR)=j\omega\rho_0 e^{-jkR}/2\pi R$ in the far field (i.e., for kR ? 1) and k_x, k_y are given in terms of spherical coordinates, i.e., $k_x=k\cos\phi\sin\theta$ and $k_y=k\sin\phi\sin\theta$ (see Figure 4). The relations between the sensor position on the hemisphere and the projected sensor position on the source plane can be defined by the coordinates $X=R\cos\phi\sin\theta$, $Y=R\sin\phi\sin\theta$, and $Z=R\cos\theta$. By using these relationships, the exponential term in equation (13) can be written as

$$e^{j(k_x x+k_y y)}=e^{j(k\cos\phi\sin\theta x+k\sin\phi\sin\theta y)}=e^{j\left(\frac{kX}{R}x+\frac{kY}{R}y\right)}. \tag{14}$$

Similarly to the case of the hemi-cylindrical sensor array, the M-by-N planar source array is assumed to have equal inter-source spacings r_{ssx} $(=L_{sx}/M)$ and r_{ssy} $(=L_{sy}/N)$ in the intervals $[-L_{sx}/2,\ L_{sx}/2]$ and $[-L_{sy}/2,\ L_{sy}/2]$ respectively and the spatial sampling points in these intervals are assumed to be defined as

$$\begin{aligned} x_m &= -\left(\frac{L_{sx}-r_{ssx}}{2}\right)+mr_{ssx}, \quad m=0,\ 1,\ \cdots\cdots,\ M-1 \\ y_n &= -\left(\frac{L_{sy}-r_{ssy}}{2}\right)+nr_{ssy}, \quad n=0,\ 1,\ \cdots\cdots,\ N-1 \end{aligned} \tag{15}$$

Under these conditions, the two-dimensional discrete Fourier transform of the spatially sampled source strength can be expressed in the form

$$U_z(k_x,k_y)=\frac{1}{\sqrt{M}}\sum_{m=0}^{M-1}\left[\frac{1}{\sqrt{N}}\sum_{n=0}^{N-1}u_z(x_m,y_n)\,e^{jk\frac{nY}{R}r_{ssy}}\right]e^{jk\frac{mX}{R}r_{ssx}} \tag{16}$$

When the acoustic pressures are assumed to be sampled at equal increments of X/R and Y/R, $k_x = kX/R$ and $k_y = kY/R$ where X and Y define the coordinates of a field point in the source plane. With the sensor geometry depicted in Figure 5(a) consisting of an $M \times N$ array whose projection on the source plane is a rectangle of dimensions L_x and L_y (i.e., $X_s = L_x/M$ and $Y_s = L_y/N$) then $\Delta k_x = kX_s/R$ and $\Delta k_y = kY_s/R$. It then follows that $\Delta k_x r_{ssx} = 2\pi/M$ for an inter-source spacing $r_{ssx} = (R/L_x)\lambda$ and also that $\Delta k_y r_{ssy} = 2\pi/N$ provided that $r_{ssy} = (R/L_y)\lambda$. Under these conditions, the exponential term in equation (16) can be written as

$$e^{jk\left(\frac{muX}{R}r_{ssx}+\frac{nY}{R}r_{ssy}\right)} = e^{jk\left(muX_s r_{ssx}+nvY_s r_{ssy}\right)} = e^{jk\left(\frac{muL_x}{RM}r_{ssx}+\frac{nvL_y}{RN}r_{ssy}\right)}, \qquad (17)$$

where u and v are the index associated with each discrete spatial frequency chosen. The discrete variable u ranges from 0 to $M-1$, and v vary from 0 to $N-1$. The superscript terms in equation (17) will become equal to $j2\pi(mu/M + nv/N)$, provided that the inter-source spacings r_{ssx} and r_{ssy} are equal to $(R/L_x)\lambda$ and $(R/L_y)\lambda$ respectively. Therefore, the final expression for the acoustic pressures in the far field at each of $u(2\pi m/M)$ and $v(2\pi n/N)$ values of the spatial frequency can be written as

$$p(u\Delta k_x, v\Delta k_y) = G_s(kR)\sum_{m=0}^{M-1}\sum_{n=0}^{N-1} u_z(x_m, y_n)\left(\frac{e^{j2\pi\left(\frac{nv}{N}\right)}}{\sqrt{N}}\right)\frac{e^{j2\pi\left(\frac{mu}{M}\right)}}{\sqrt{M}}, \qquad (18)$$

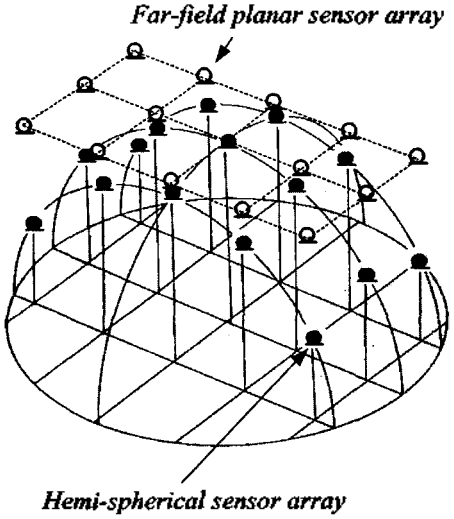

(a) The hemi-spherical sensor array and the far-field planar sensor array.

and the far field pressure is exactly a two dimensional discrete Fourier transform of the source distribution. It should be emphasised that the above relationship of the discrete Fourier transform holds only when the separation of acoustic sources r_{ssx} and r_{ssy} are equal respectively to $(R/L_x)\lambda$ and $(R/L_y)\lambda$. Therefore, the matrix of Green functions relating the composite vector of far field pressures at the sensors to the composite vector of source strengths defined by

$$\mathbf{G}_{DS} = G_s(kR)\mathbf{W}_B, \qquad (19)$$

where the block matrix $\mathbf{W}_B$ is given by

$$\mathbf{W}_B = \frac{1}{\sqrt{M}}\begin{bmatrix} [\mathrm{w}] & [\mathrm{w}] & \mathrm{g} & [\mathrm{w}] & [\mathrm{w}] \\ [\mathrm{w}] & w_m[\mathrm{w}] & \mathrm{g} & w_m^{M-2}[\mathrm{w}] & w_m^{M-1}[\mathrm{w}] \\ \mathrm{g} & \mathrm{g} & \mathrm{g} & \mathrm{g} & \mathrm{g} \\ [\mathrm{w}] & w_m^{M-2}[\mathrm{w}] & \mathrm{g} & w_m^{(M-2)(M-2)}[\mathrm{w}] & w_m^{(M-2)(M-1)}[\mathrm{w}] \\ [\mathrm{w}] & w_m^{M-1}[\mathrm{w}] & \mathrm{g} & w_m^{(M-1)(M-2)}[\mathrm{w}] & w_m^{(M-1)(M-1)}[\mathrm{w}] \end{bmatrix}, \qquad (20)$$

where $w_m = e^{j(2\pi/M)}$ and each $N \times N$ sub-matrix $\mathbf{W}$ is equal to the Fourier matrix from equation (12). The block matrix $\mathbf{W}_B$ also has the same pattern of the Fourier matrix $\mathbf{W}$ and, interestingly, the condition number is unity since all the singular values of the matrix $\mathbf{W}_B$ are unity.

Similarly to the two-dimensional case, the problem does not become optimally conditioned, as shown in Figure 5(b), when using a planar type of sensor array as depicted in

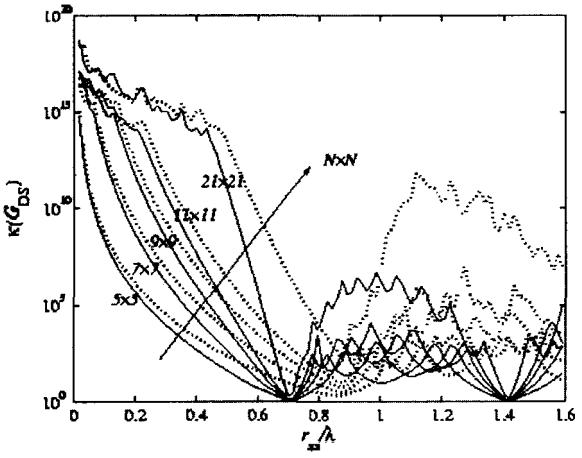

(b) Variation of the condition number for the hemi-spherical sensor array (solid line) and the far-field planar sensor array (dotted line) for a range of numbers of N-by-N sensors and sources

Figure 5. The hemi-spherical sensor array and the far-field planar sensor array, when $R = 10^3 r_{ss}$.

Figure 5(a). This has the same inter-sensor spacing r_{mm} as that of the hemi-spherical sensor array, but the conditioning of the matrix $\mathbf{G}_{DS}$ for the far-filed planar sensor array becomes much poorer as the assumed number of sensors and sources increases. However, by the adoption of the hemi-spherical sensor array, the conditioning of the matrix $\mathbf{G}_{DS}$ is greatly improved and becomes optimal when $r_{ss} = \lambda/\sqrt{2}$ (when $r_{ms} = 10^3 r_{ss}$), irrespective of any range of $M \times N$ sources and sensors assumed. Hence, the inversion of the matrix $\mathbf{G}_{DS}$ is consequently the least sensitive to errors under this condition.

V. Conclusions

As a result of this investigation of the factors determining the conditioning of the matrix $\mathbf{G}$, it has been shown that the conditioning of the acoustical inverse problem is highly dependent on the geometry of sources and measurement positions and the frequency of the radiated sound. It has also been demonstrated that the acoustical inverse problem can become the best conditioned when the sensor and source geometry is optimally arranged, even when the sensor array has been completely deployed to the far field. This will enable guidelines to be proposed for source and sensor geometries that reduce sensitivities to various kinds of errors. The source and sensor array suggested may also be helpful in achieving better estimate of strengths of acoustic sources.

References

1. P.A. Nelson, "A review of some inverse problems in acoustics," *International Journal of Acoustics and Vibration* 6(3), 118-134, 2001.
2. Y. Kim, "Spatial resolution limits for the reconstruction of acoustic source distribution by inverse techniques," PhD Thesis, University of Southampton, 2002.
3. S. Barnett, *Matrices: methods and applications*, Clarendon Press, Oxford, 1990.
4. A.P. Dowling and J.E. Ffowcs-Williams, *Sound and Sources of Sound*, Ellis Horwood, Chichester, 1983.
5. P.A. Nelson and S.J. Elliott, *Active control of sound*, Academic Press, San Diego, 1992.
6. K.R. Castleman, *Digital image processing*, Prentice Hall, New Jersey, 1996.
7. P.M. Morse and K.U. Ingard, *Theoretical Acoustics*, Princeton University Press, New Jersey, 1968.

[Profile]

● Youngtea Kim

Youngtae Kim graduated in Mechanical Engineering from Korea University in 1988. Following this completed a Masters degree in Fluid and Thermal Engineering at the Mechanical Engineering Department at Korea University. From 1990 he worked for 9 years in Daewoo Motor Company on Flow and NVH analysis before returning to the Institute of Sound and Vibration Research (ISVR) at the University of Southampton (United Kingdom) to begin a PhD. This was awarded in 2003 for work on the spatial resolution limits in acoustical inverse problems. He then moved to Samsung Advanced Institute of Technology (SAIT, Korea) to work on virtual acoustics project, and is currently Principal Researcher in Computational Science & Engineering (CSE) Lab. He is undertaking research into virtual acoustics and active flow-induced noise control.